Appl Biochem Biotechnol (2016) 178:725–738
DOI 10.1007/s12010-015-1905-7

Rational Substitution of Surface Acidic Residues for Enhancing the Thermostability of Thermolysin

Fucheng Zhu[1] · Yu Zhuang[1] · Bin Wu[1] · Jiahuang Li[3] · Bingfang He[1,2]

Received: 29 July 2015 / Accepted: 21 October 2015 /
Published online: 29 October 2015

Abstract Solvent-exposed acidic/amide residue (Asp/Glu or Asn/Gln) exerts great effects on the thermostability of protein; however, experimental attempts appear to be time-consuming, so a more scientific, simple, and effective rational strategy is necessary. In this study, molecular dynamic (MD) simulation was performed to analyze two surface acidic residues (Asp37 and Glu119) of thermolysin (TLN) in mediating its thermostability. Root-mean-square-deviation (RMSD) was calculated to evaluate the thermosensitivity effect by acidic/amide substitutions. The wild-type TLN and three mutants (TLM1, TLM2, and TLM) presented significantly different thermostability effect. Four profiles of RMSD values demonstrated that the thermal insensitivity of variants were TLM2>TLM>TLN>TLM1. As expected, the thermostability and half-life (at 60 °C) behavior of enzyme variants showed the same trends with the computational predictions, and it was worth noting that the half-life of TLM2 showed 3.1-fold longer than that of wild-type. The T_m and T_{50} of TLM2 were 9 and 7 °C higher, respectively, than that of wild-type enzyme. Rational substitution of acidic/amide residue in regulation of thermostability using MD simulation would be an efficient approach for instructional design to improve the thermostability.

Electronic supplementary material The online version of this article (doi:10.1007/s12010-015-1905-7) contains supplementary material, which is available to authorized users.

✉ Jiahuang Li
lijiah@nju.edu.cn

✉ Bingfang He
bingfanghe@njtech.edu.cn

[1] College of Biotechnology and Pharmaceutical Engineering, Nanjing Tech University, 30 Puzhunan Road, Nanjing 211816, China

[2] School of Pharmaceutical Sciences, Nanjing Tech University, 30 Puzhunan Road, Nanjing 211816, China

[3] State Key Laboratory of Pharmaceutical Biotechnology, College of Life Sciences, Nanjing University, Nanjing 210093, China

Keywords Surface acidic residue · Thermostability · Molecular dynamic simulation · Thermolysin

Introduction

Enzyme thermostabilization is an important issue in biotechnology research due to the potential benefits in industrial applications [1]. In the past years, some efforts have been found that substitution of Asp/Glu by its neutral isosteric Asn/Gln residues usually significantly alteration of its thermostability. For example, Irún and his coworkers [2] reported that substituting acidic residue with amide residue significantly enhanced the thermostability of apoflavodoxin. The thermostability of xylanase improved over 1.5-fold than that of wild-type by D137N substitution according to Xue et al. [3]. While, some mutagenesis shown no or even reduction of thermostability though substitution of Glu or Asp by its corresponding amide residue according to report [4]. The difficulties in prediction of acidic/amide amino acid mutation effect is that they share similar structure and properties. In addition, large number of acidic/amide amino acid usually exiting in enzyme makes it hard to select and evaluate its stabilizing effect, positive, negative, or no obviously effect, because experimental attempts in mutation particular multipoint mutation are time- and labor-consuming. Therefore, further development of an effective strategy by combining multiple structural features rather than a single factor is necessary.

To date, several structural features are known to play important factor in enzyme stability. Many successful rational designs are based on protein-core modifications [5, 6]. Intramolecular design, however, usually results in reduction or even complete inactivation in enzymatic activity [5]. Protein surface has an importance in protein thermostability that has not been investigated sufficiently, which has attracted more attention to focus on it especially combining with flexible region [7, 8]. There is currently a better understanding of the loop domain having higher flexibility, which is critical for protein thermostability [9]. Molecular dynamic (MD) simulation is an efficient approach for evaluation of enzymatic stability effect [10–12]. Generally, thermophile enzymes are more rigid and stable with lower root-mean-square-deviation (RMSD) values than mesophile ones [11]. The rationale is that conformation with higher RMSD is more likely to unfold in an early stage, and that substitutions at the specific site have a higher chance to stabilize the folded state as enhancing intramolecular interactions and present lower RMSD value, such as hydrogen bond interactions or hydrophobic interactions [13–15]. Therefore, lowering the overall RMSD is one way to identify mutation with more stability.

In this study, we used the thermolysin (TLN) as model enzyme. TLN is an efficient industrial enzyme for synthesis of peptides, such as precursor of an artificial sweetener aspartame [16] and a typical template for thermostability studies [17–19]. Despite the wealth of information that has been gathered on the influence of mutations on enzyme thermostability, few systematic studies have predicted the stabilizing effect of those acidic/amide residue mutations. Besides, the thermostability of TLN needs further improvement because it is not great stable when in presence of buffer without calcium ion [20]. Here, rational design strategy was used to selected and identified target site effects. Surface acidic residue located in loop region was considered as the target mutagenesis sites, and then submitted to investigate the thermostability mediated by substitution of acidic residues with its corresponding amide type. As a result, more thermostable mutants of TLN were constructed successfully without

hampering catalytic activity. Furthermore, thermoduric mechanisms underlying this substitution were investigated by analysis of the overall structural changes, dynamics, and the local conformational changes around mutation residue. It is helpful not only for the design of thermostable proteins but also for comprehensive understanding of the role of surface acidic/amide residues in enzyme thermostability.

Materials and Methods

Bacterial Strains, Plasmids, and Materials

Bacillus subtillis WB800 and modified plasmid pMA05 (supplied by Jiangnan University) were used as host and vector, respectively, for *npr* gene cloning and expression [21]. The *npr* gene encoding thermolysin and the primers were synthesized by Invitrogen (Shanghai, China) according to reported in GenBank database (accesssion number X76986.1). The plasmid mini kit and a gel extraction kit were obtained from Axygene (Hangzhou, China). T4 DNA ligase, DNA polymerase, and restriction enzymes were purchased from Takara (Tokyo, Japan). All other chemical reagents were obtained from Sigma-Aldrich (St. Louis, MO, USA).

Computational Modeling

The crystal structure of TLN determined by Holland et al. at 1.70 Å resolution (PDB code: 1LNF) was used for the simulations [22]. The in silico design of the mutants was created using the Discovery Studio 4.0 package followed by energy minimization. The crystallographic water molecules were retained to mimic a hydration shell. MD simulation was performed using Gromacs version 4.5 with the GROMOS 53A6 force field [23]. The conjugate was solvated by explicit water using a simple point charge (SPC) model [24], and sodium ions was added to neutralize the system. The electro-neutral systems were subjected to a steepest descent energy minimization, and then the 500-ps MD simulation was performed with the heavy atoms and protein fixed. Lastly, a 20-ns MD simulation was performed on the entire system in a temperature gradient (300 and 380 K). All of the bond lengths were constrained using the LINCS algorithm [25]. The cutoff value for the van der Waals interactions was set at 1.0 nm, and the electrostatic interactions were calculated using a particle mesh Ewald algorithm. Periodic boundary conditions were used, and the coordinates were saved for analysis every 1 ps. The trajectory analysis was performed using standard Gromacs tools. PyMOL0.99rc6 and VMD1.91 were used to analyze the structures and trajectories.

Construction and Preparation of Thermolysin Variants

The 1563-bp fragment which is encoding pro-peptide and mature-peptide of *npr* gene was amplified using the oligonucleotides TLN-F (5′-GCGGGAATTCTCAACGGAACACGTTACA-3′) and TLN-R (5′-AATGTCGACTTATTTCACCC CTACCGCATCA-3′), digested by EcoRI and SalI and inserted in pMA05, and then transformed into *Escherichia coli* DH5α. TLM1(D37N), TLM2(E119Q), and TLM(D37N/E119Q) mutants were generated using the QuikChange™ Site-Directed Mutagenesis Kit (Stratagene, La Jolla, CA). The gene site-saturation mutagenesis libraries were also generated using the QuikChange™ Site-Directed Mutagenesis Kit

(Stratagene, La Jolla, CA). The mutation site was designed as NNK (N, adenine/cytosine/guanine/thymine; K, guanine/thymine), and the recombinant plasmid was used to transform into *E. coli* BL21. The clones with clear zone in agar plate containing milk were selected and verified by sequencing (GenScript, Nanjing). All primers used in this study are shown in Table S1 in supplementary information.

The plasmid harboring the insert gene was transformed into an expression host, *B. subtillis* WB800. An overnight culture (1 mL) of recombinant *B. subtillis* WB800 in TB medium containing kanamycin (50 μg/mL) was inoculated into 100 mL Terrific Broth medium containing kanamycin (50 μg/mL) and incubated at 37 °C, 180 rpm for 24 h. The culture supernatant was obtained by centrifugation and loaded on a DEAE-Sepharose fast-flow column, pre-equilibrated with 50 mM Tris–HCl (pH 8.0). The unabsorbed protein fractions were eluted with the same buffer at a flow rate of 1 mL/min. The eluted fractions were tested for its protease activity as described previously and the fraction displaying protease activity was concentrated by centrifugation using a Centricon 10-kDa molecular weight cutoff device (Millipore, USA), and then the purity was analyzed using 12 % (*v/v*) SDS-PAGE and the protein content was assayed by Bradford's method with BSA as the standard.

Determination of Kinetic Parameters

Protease activity was measured as described previously [26]. Two milliliters of sample was added to the solution (2 mL) containing 2 % (*w/v*) casein and 50 mM Tris–HCl buffer (pH 8.0). The reaction mixture was incubated at 40 °C for 10 min and terminated by the addition of 4.0 mL TCA mixture (containing 0.11 M trichloroacetic acid, 0.22 M sodium acetate, and 0.33 M acetic acid). This mixture was further centrifuged at 15,000×*g* for 15 min, and the absorbance of resulting supernatant was measured at 280 nm against a blank control. One unit (U) of protease activity was defined as the amount of enzyme that hydrolyzed the casein and produced 1 μg of tyrosine per min under the assay conditions.

K_m and k_{cat} values were assessed by measuring the proteolytic activity on casein as a substrate. The activities were measured at a fix concentration of purified enzyme (0.15 mg·mL^{-1}) and by varying the concentrations of casein, ranging from 0.5 to 10 mg·mL^{-1}. Non-linear regression method (Origin Pro 8.5) was used to fit experimental kinetic curves. All of the experiments were performed in triplicates.

Measurement of Thermal Stability

To detect thermostability (T_{50}) of the enzyme, the TLN variants were incubated in 50 mM Tris–HCl buffer (pH 8.0) at 30–70 °C for 1 h, and aliquots were withdrawn and cooled on ice for 10 min. The residual activities of the enzymes were measured at 40 °C as previously described. T_{50} was defined as the temperature at which the enzyme activity was reduced by half during 1 h of incubation.

To measure the half-lives ($T_{1/2}$) of thermolysin variants, enzyme samples were incubated at 60 °C for different durations (0, 20, 40, 60, 90, 120, 150, 180 min) then kept on ice for 10 min. Subsequently, the residual activities were determined as described previously. In all assay solutions, the final concentrations of samples were equal quantities. All above assays were performed in triplicate.

Circular Dichroism Measurements

Circular dichroism (CD) measurements for the wild-type (WT) and mutant enzymes were performed with Chirascan-plus Circular Dichroism spectrometer (Applied Photophysics, UK) equipped with a computer-controlled thermostat. Spectra were recorded from 190 to 260 nm using a 1-mm cell and a bandwidth of 1 nm. Unfolding curves were measured at 222 nm from 30 to 90 °C using the temperature scan mode with a gradient of 1 °C/min, and measurements were performed in 5 mM Tris–HCl buffer (pH 8.0) using protein concentration of 4 μM.

Results and Discussion

Selection and Identification of Target Residues

Acidic residue (Asp and Glu) was recognized as a promising target for protein thermostabilization in our study. Considering that protein surface with less specific interactions was safer as good candidates for engineering thermostability without hampering catalytic activity or other enzyme features, we investigated the surface acidic residue located in N-terminal loop of TLN for further research, as this region of TLN plays an important role in stabilization [27]. Four residues Asp37, Asp57, Asp59, and Glu119 were identified. However, two residues Asp57 and Asp59 have interaction with calcium ion of TLN [20]. In view of the effect of site-directed mutagenesis on the interaction of calcium ion binding region, only Asp37 and Glu119 were selected as hot spots for subsequently MD simulations and site-directed mutagenesis.

Unfolding MD Simulations

In order to compare the thermostability of the native TLN and the corresponding mutated systems TLM1(D37N), TLM2(E119Q), and TLM(D37N/E119Q), the unfolding simulations were addressed in 20-ns MD simulations at 380 K. The simulations were started from the optimized structure obtained at the balanced trajectories of the 300-K simulations. In Fig. 1, the RMSD (Cα atoms) values from initial conformations of wild-type and mutants at 380 K were given. At this high temperature, TLM2 and TLM were more stable than TLN and TLM1. At the end of simulation, TLM2 and TLM reached balance and stabilized around at 4.8 and 5.5 Å, respectively. By comparison, TLN and TLM1 peaked at 8.7 and 9.6 Å and kept its upward trend. Common stabilizing strategies, such as introducing disulfide bonds or salt bridges and enhancing intramolecular interactions, always lead to a decrease in the overall RMSD value of an enzyme [28–30]. Generally, lower RMSD represents a better initial conformational preservation of enzyme structure and consequently higher thermostability. Therefore, the thermolysin variants showed the possible following order of increasing thermostability: TLM2>TLM>TLN>TLM1.

Protein Flexibility of TLN and Variants

To benchmark the high-temperature unfolding, MD simulations were carried out at 300 K for the native TLN and the corresponding variants. RMSD values presents that all enzymes

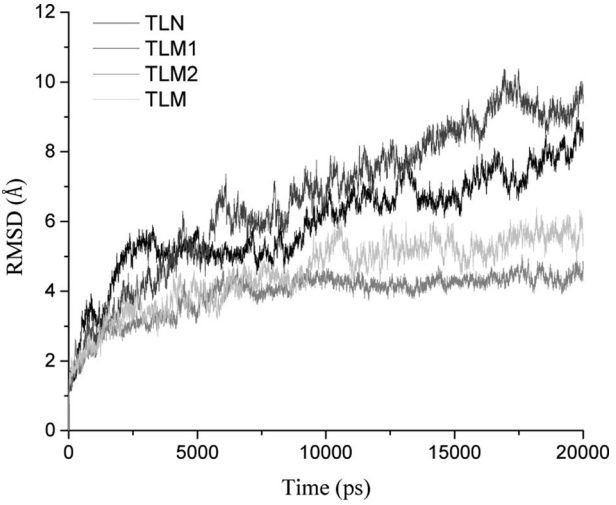

Fig. 1 Root mean squared deviations (RMSDs) of the Cα atoms for the thermolysin and the three mutants over all trajectories in the 380 K (20 ns)

reached balance at last 5 ns (Fig. 2). In general, the mutants TLM2 and TLM are more stable than TLN and TLM1, which is in line with the result of unfolding simulations.

Protein flexibility is known as an important role in modulating stability of enzymes. For example, Liu et al. [11] compared two nitrile hydratases from different sources and identified that lower flexibility of enzyme is promising to markedly increase their thermal stability. In particular, earlier attempts, which succeed in thermostabilizing enzyme by reducing flexibility of both surface and cavity residue, revealed that flexibility was a useful indicator of thermostabilization of enzyme [31–33].

To gain insight into flexibility, we compared the average RMS fluctuations of each residue from last 5-ns simulations. As shown in Fig. 2, the flexibility of the systems is quite similar with slight difference in region of N-terminal and active center. The average of the Cα

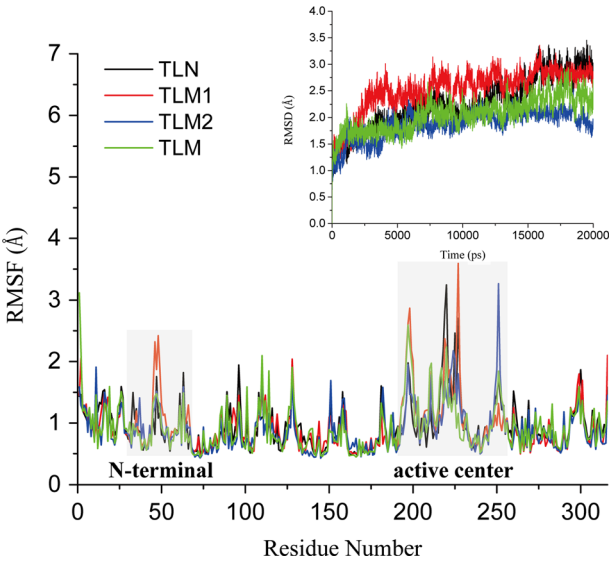

Fig. 2 RMSDs of the Cα atoms for the thermolysin and the three mutants over all trajectories in the 300 K (20 ns); the average RMSF calculated from last 5 ns for thermolysin variants

fluctuations at 300 K for the wild-type of the TLN and the mutant systems is small (0.864, 0.968, 0.815, and 0.849 Å) and the results follow this trend TLM1>TLN>TLM>TLM2.

Analysis of Interaction Around Mutagenesis Sites

By using MD simulations, the mutants in thermostability effects were identified efficiently. There are multiple factors that can influence protein thermostability, such as hydrophobic interactions, packing efficiency, amino acid composition, salt bridges, hydrogen-binding networks, and hydrated shell around protein surface [34–36]. To investigate the structural effects of these mutations, interaction around mutagenesis sites including intramolecular and intermolecular interaction might be used to understand the impact of mutations on the structure of thermostability. Two mutagenesis residues were analyzed as follows.

To assess the contribution of Asp37→Asn to the decrease of thermostability, the wild-type TLN and TLM1 mutant were compared. Table 1 shows that occupancy and distance of hydrogen bonds formed around Asp37 in TLN model and Asn37 in TLM1 model is quite similar, demonstrating alteration of thermostability at residue 37 substitution has no correlation with hydrogen bond. Hydrated shell around protein has been shown to be related to the thermostability according to our previous report [37]. Spherically averaged densities of water in the mutagenesis residue as a function of the distance from the residue center were also detected from trajectories of last 5-ns MD simulations. As shown in Fig. 3b, water density around the Asp37 in TLN model is higher than that around the Asn37 in TLM1 model, indicating the well-hydrated state of the enzyme with Asp37; however, the similar difference has not been detected from TLN and mutant E119Q. Superposition of average conformation indicates that the structures of Asp and Asn at position 37 were essentially identical other than carboxyl group of side-chain of Asp37 (Fig. 3a). The Asp37 have three hydrogen bonds (H-bond) including interaction with Asn97 and two another water molecules. Compare with Asp37, the Asn37 has a movement into intramolecular of enzyme, which impairs interaction of β-$CONH_2$ of Asn37 and water molecule. Substitution of Asp37 to Asn likely reduced the capacity of binding water of this region, resulting in a hydrated shell decrease for the enzyme and decreasing its thermostability.

Glu119 is partially buried. The conformation of Gln119 in TLM2 model is similar to wild-type (Fig. 3c) beside the group $CONH_2$ of Gln119, and Fig. 3d shows that no significant hydrated shell alteration around position 119 between TLN and TLM2 mutant is observed, suggesting that, contrary to D37N mutant, E119Q mutant have no effect on hydrated shell. Structure analysis indicated that only the atom OE_2 of Glu119 was surface exposed and the region around Glu119 is highly bulky hydrophobic residues(Phe40, Tyr42, Leu50, Pro51, Tyr93, Tyr106, Tyr110, Phe114, Trp115, and Try122) (Fig. 4a). Hydrophobic cluster has been

Table 1 Occupancy and distance of hydrogen bond data collect along MD simulations

Donor H-X	Acceptor	Occupancy (%)	Distance (Å)	Donor H-X	Acceptor	Occupancy (%)	Distance (Å)
Asp37.N	Asn97.O	53.1	3.0±0.2	Asn37.N	Asn97.O	52.2	3.1±0.2
Ser103.OG	Glu119.OE1	60.3	2.8±0.1	Ser103.OG	Gln119.OE1	76.8	2.8±0.1
Asn116.N	Glu119.O	54.0	3.0±0.2	Asn116.N	Gln119.O	53.8	3.0±0.2
Glu119.N	Asn116.OD1	63.0	2.9±0.1	Gln119.N	Asn116.OD1	70.3	2.9±0.1

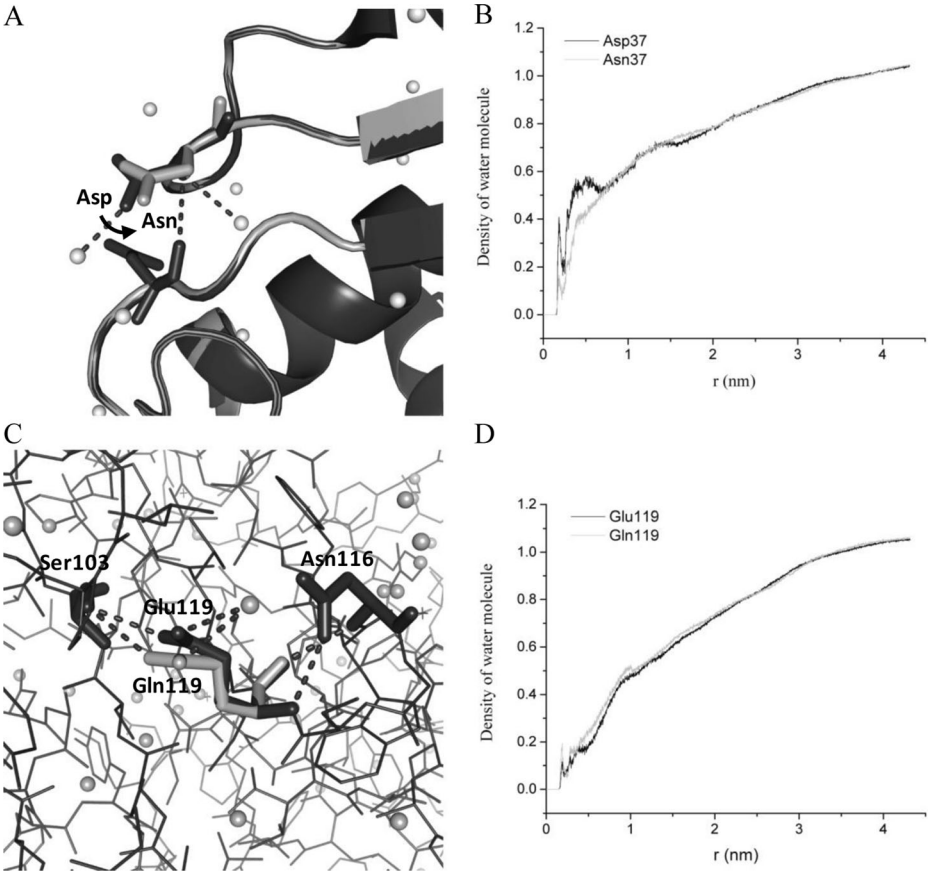

Fig. 3 Stereo views of the residues and their surroundings at the mutant sites before (**a**, **c**) and after mutation. Spherically averaged number densities of water molecules as a function of distance from the around mutagenesis sites 37 (**b**) and 119 (**d**). Water molecular were labeled in *gray sphere*

reported to have greater benefit for thermostability [38]. As the p*K*a of the γ-COOH of Glu is 4.1, the Glu119 is deprotonated and charged at physiological conditions. It is generally assumed that charged residues are not favorable at interior sites for protein stability. In this study, the charged Glu119 go against stabilizing local hydrophobic cluster. Conversely, glutamine amide moiety, without dissociative behavior, thus decreases disruption of compactness of local hydrophobic cluster and maintains its hydrophobicity towards aqueous environment. In order to further determine the effect of E119Q on this hydrophobic cluster, the compactness of this cluster was analyzed using radius of gyration along the MD simulation. As shown in Fig. 4b, the cluster in the Gln119 model is lower than Glu119 model along the whole simulation, indicating that the hydrophobic cluster around the Gln119 is well compact. Additionally, both Glu119 and Gln119 at this position were involved in hydrogen bonding with Ser103 or Asn116. The occupancy of all discussed hydrogen bond was calculated from trajectories of last 5-ns MD simulations. As shown in Table 1, the hydrogen bond between Gln119 and Ser103 or Asp116 is enhanced compared with Glu119 as occupancy value increased from 60.3 to 76.8 % and from 63.0 to 70.3 %, respectively. This result is consistent with previous reports that strength of hydrogen bonding interaction between neutral amino

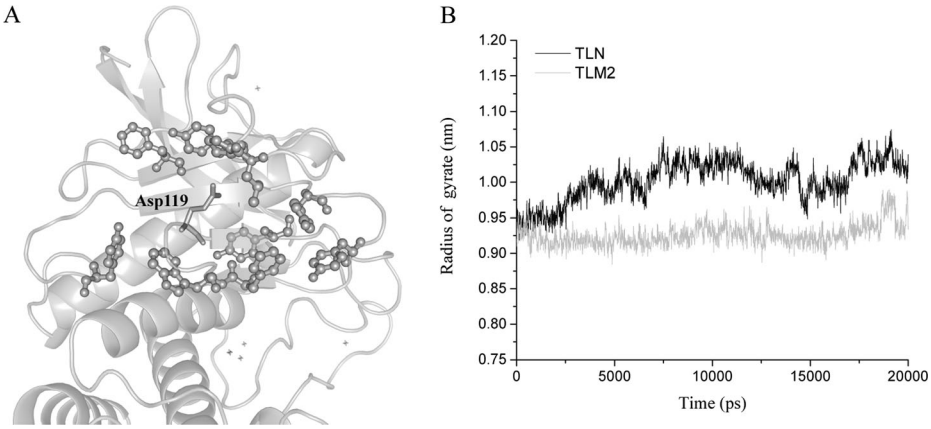

Fig. 4 Stereo views of hydrophobic cluster around Asp119 (**a**); radius of gyration of hydrophobic cluster in TLN and TLM2 model over all trajectories in the 300 K (20 ns) (**b**)

acids is stronger than charged one [39]. Menach et al., via site-directed mutagenesis of Asn116, confirmed that the N-terminal β-hairpin structure, Asn112-Tyr122, plays an important role on activity and stability of TLN [40]. As an important hydrogen bonding participated in this β-hairpin structure, the enhanced interaction network around Gln119 is beneficial for stabilizing this β-hairpin structure compared with Glu119. In general, the Gln119 not only reduced interruption of electrostatic potential energy to hydrophobic cluster but also introduced a relatively compact conformation and maintained the native-like microenvironment near the active center though optimize favorable intramolecular interactions to stabilize the activity at high temperature.

Expression and Structural Characterization of Thermolysin Variants

To verify computational prediction of mutations in mediating thermal stability of TLN, we conducted recombinant experiment of aforementioned mutants by site-direct mutagenesis. New mutants were successfully constructed, expressed in *B. subtillis* WB800 and secreted into the culture medium. The activity of TLN and all mutants in culture supernatant reached to the relative highest proteolysis activity of 800–1000 U/mL after cultured for 24 h. The result revealed that the mutation has little effect in enzyme expression and activity (data not shown). On the other hand, the CD spectra of mutants showed similar in pattern and intensity to the WT enzyme (TLN) as shown in Fig. 5, indicating that the mutations did not significantly affect the structure domain of the protein.

Thermostability and Kinetic Characterization of Thermolysin Variants

Previous several studies have revealed that calcium ion has a critical importance in thermostability of TLN [20, 37]. Considering single factor variable and ignoring the possible interaction between the Ca^{2+} and mutation, here, we performed the experiment with enzymes in presence of the buffer without calcium ion. The thermostability of purified thermolysin from wild-type or mutants was quantitatively characterized by T_{50} value as shown in Table 2. After 60 min of incubation, the T_{50} values of thermolysin variants were TLM2>TLM>TLN> TLM1. Surface acidic/amide residues substitutions in thermostability effect were conformed

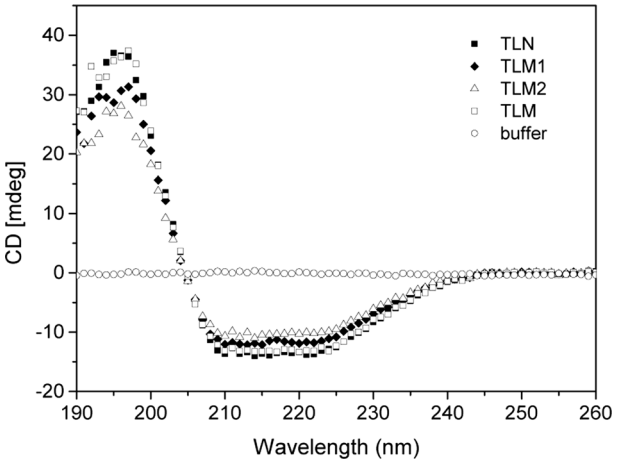

Fig. 5 Far-UV circular dichroism (CD) spectra of wild-type and mutants at 30 °C

and the biggest difference value in melting temperature (T_{50}) of mutant and wild-type was 11 °C. Two mutants TLM and TLM2 were improved to be more stable. The substitution to Gln at residue 119 conferred the highest thermostability. At residue 37, substitution to Asn showed an adverse stabilization effect.

To further investigate the thermostability of enzymes, wild-type and three mutants were incubated at 60 °C for 3 h in Tris–HCl buffer (pH 8.0, without calcium ion), respectively. As shown in Fig. 6, after 60 min of incubation, only 20–30 % activity of the wild-type protein retained after heat treatment. TLM and TLM2 mutants showed a higher thermostability than the wild-type protein with nearly 70 % residual activity, while the mutants TLM1 showed reduced thermostability lower than 20 % residual activity. TLM and TLM2 mutants displayed significantly longer half-lives at 60 °C, 90.0 min for TLM and 110.6 min for TLM2, which were 2.9- and 3.6-fold greater than that of wild-type TLN (30.8 min), respectively. However, TLM1 mutant (19.9 min) was only 0.64-fold of wild-type at 60 °C. These in vitro experiments strongly validated the prediction presented in this research.

The kinetic constants were also determined as shown in Table 2. Usually, thermostability enhancement of enzyme is accompanied by the impairment of catalytic activity. Fortunately, the similar rule was not observed in our research as shown in Table 2. For TLM2 mutant, although there was a significant improvement in thermostability, no compromise of catalytic activity (k_{cat}/K_m) was observed. The catalytic constant k_{cat} of TLM2 was considerable high.

Table 2 Thermostability and kinetic constants of the wild-type TLN and mutants

Thermolysin variants	Amino acid changes	Melting temperature (T_{50}) (°C)[a]	Half-lives[b] ($T_{1/2}$) (min)	K_m[c] (mg·mL^{-1})	k_{cat}/K_m[c] (mL mg^{-1}·min^{-1})
TLN	None	55.1±0.2	30.8±0.1	3.8±0.12	2.37±0.015
TLM1	D37N	51.7±0.2	19.9±0.2	3.6±0.11	2.0±0.009
TLM2	E119Q	62.1±0.1	110.6±0.3	5.4±0.16	2.25±0.013
TLM	D37N/E119Q	61.2±0.3	90.0±0.2	4.0±0.13	2.26±0.012

[a] T_{50} represents the temperature at which the enzyme activity was reduced by half during 1 h of incubation

[b] $T_{1/2}$ is the half-life of thermolysin variants at 60 °C

[c] Kinetic constants were calculated according to fitting line in the supplementary information (Fig. S1)

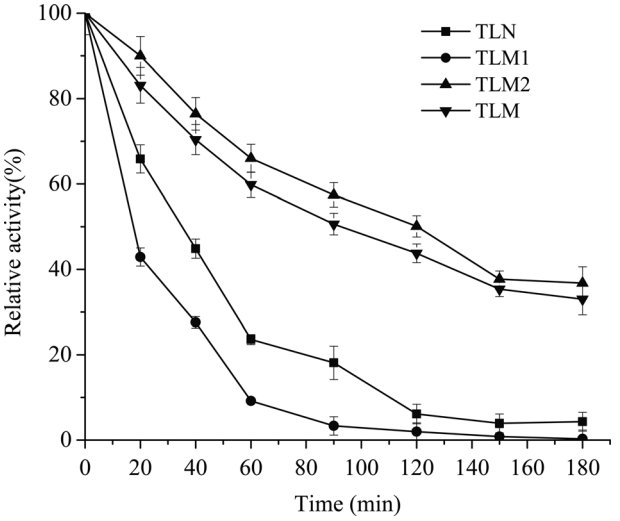

Fig. 6 Thermostability of wild-type TLN and mutants. The residual activities of the enzymes were determined after incubating at 60 °C and pH 8.0 for different interval times. The initial activity of each enzyme was defied as 100 %. Data are presented as mean ±SD (n=3)

The K_m of TLM2, however, slightly increased from 3.8±0.12 mg·mL^{-1} of TLN to 5.4± 0.16 mg·mL^{-1}, suggesting a decrease in the affinity towards casein; this could be partly responsible for the similar the ratio of k_{cat}/K_m with that of wild-type TLN. Meanwhile, the TLM1 and TLM mutants kept the similar catalysis properties both in k_{cat}/K_m and K_m to that of wild-type TLN, suggesting these selected substitutions did not alter the catalytic activity.

The results from experiments and MD simulation suggested that 119 site played much more important role in mediating the thermostability of TLN. Thus, we conducted a site-saturation mutagenesis of 119 residue. The mutants with proteolytic activity were selected to determine thermostability at 60 °C for 1 h. The results presented that the E119Q have a highest thermostability in all of selected mutants (see Fig. S2). It was worth noting that the stability of non-charged 119 residue mutations was generally higher than that of charged one, which was coherent with demonstration in previous MD simulation.

Thermal Unfolding

The thermostability of thermolysin variants were assessed by monitoring the thermal denaturation procession using CD at 222 nm. As shown in Fig. 7, the CD signal of thermolysin variants decreased slowly as the temperature increased from 30 to 50 °C and reached its minimum at 80–90 °C. The unfold curve was scaled with the CD value at 30 °C as the native state (f_U=1) and the CD value at 90 °C as the unfold state (f_U=0). The apparent melting temperature T_m was estimated as the temperature of f_U=0.5. The wild-type enzyme TLN had a T_m value of 62 °C. Mutants TLM1, TLM2, and TLM had T_m value of 58, 71, and 68 °C, respectively. TLM2 presented the highest T_m in all mutants, nearly 10 °C of T_m increase compared with wild-type TLN. The TLM1 still had a lowest T_m value in all studied enzyme. The obtained results were also consistence with T_{50}.

Protein denaturation from any extreme environment usually results in loss of catalytic function in almost all enzymes. Heat denaturation, for instance, usually affects weak interactions such as hydrogen bonds which ultimately destabilize the native conformation of proteins. Consequently, proteins work well within a specific temperature range beyond which

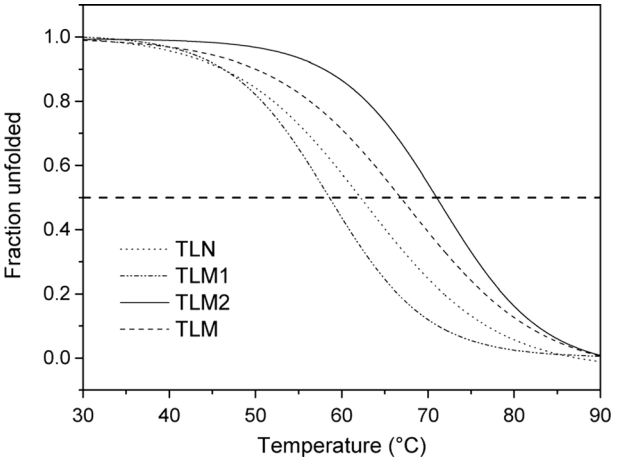

Fig. 7 Temperature-induced unfolding of thermolysin variants measured with circular dichroism spectroscopy for thermolysin variants

denaturation affects catalytic function [41]. Since the impact of heat on proteins is not easily predicted, obtaining a relatively thermal stable enzyme for a given catalytic role is extremely beneficial. In this study, mutant TLM2 displayed remarkable thermal tolerance. It is assumed that the charged substitution E119Q in TLM2 leads to an increase in structural stability of the location, and ultimately higher enzymatic stability.

Conclusions

In summary, we have successfully improved the thermostability of thermolysin through surface acidic/amide residue substitutions under the rational selection and the guidance of MD simulation. The stabilization of thermolysin and prolongation of its half-life with rational substitution of surface acidic/amide residue without decreasing its catalytic efficiency broaden the industrial applications of thermolysin. Moreover, possible explanations of the mechanisms involved in thermostability enhancement were stabilization of hydrophobic interactions cluster, intramolecular hydrogen bond interactions, and alteration of regional hydration shell.

Acknowledgments This work was supported by the National Program on Key Basic Research Project (2011CBA00807), the National High Technology Research and Development Key Program of China (2012AA022205), and KYZZ_0228 from Jiangsu Province.

References

1. Fágáin, C. Ó. (1995). Understanding and increasing protein stability. *Biochimica Et Biophysica Acta-Protein Structure and Molecular Enzymology, 1252*, 1–14.
2. Irun, M. P., Maldonado, S., & Sancho, J. (2001). Stabilization of apoflavodoxin by replacing hydrogen-bonded charged Asp or Glu residues by the neutral isosteric Asn or Gln. *Protein Engineering, 14*, 173–181.
3. Xue, H. P., Zhou, J. G., You, C., Huang, Q., & Lu, H. (2012). Amino acid substitutions in the N-terminus, cord and alpha-helix domains improved the thermostability of a family 11 xylanase XynR8. *Journal of Industrial Microbiology & Biotechnology, 39*, 1279–1288.
4. Sanchez-Torres, P., Visser, J., & Benen, J. A. E. (2003). Identification of amino acid residues critical for catalysis and stability in *Aspergillus niger* family 1 pectin lyase A. *Biochemical Journal, 370*, 331–337.

5. Abraham, T., Pack, S. P., & Yoo, Y. J. (2005). Stabilization of *Bacillus subtilis* lipase a by increasing the residual packing. *Biocatalysis and Biotransformation, 23*, 217–224.
6. Woolfson, D. N. (2001). Core-directed protein design. *Current Opinion in Structural Biology, 11*, 464–471.
7. Kim, S. J., Lee, J. A., Joo, J. C., Yoo, Y. J., Kim, Y. H., & Song, B. K. (2010). The development of a thermostable CiP (*Coprinus cinereus* peroxidase) through in silico design. *Biotechnology Progress, 26*, 1038–1046.
8. de Kreij, A., van den Burg, B., Venema, G., Vriend, G., Eijsink, V. G. H., & Nielsen, J. E. (2002). The effects of modifying the surface charge on the catalytic activity of a thermolysin-like protease. *Journal of Biological Chemistry, 277*, 15432–15438.
9. Singh, S. K., Heng, C., Braker, J. D., Chan, V. J., Lee, C. C., Jordan, D. B., Yuan, L., & Wagschal, K. (2014). Directed evolution of GH43 beta-xylosidase XylBH43 thermal stability and L186 saturation mutagenesis. *Journal of Industrial Microbiology & Biotechnology, 41*, 489–498.
10. Akcapinar, G. B., Venturini, A., Martelli, P. L., Casadio, R., & Sezerman, U. O. (2015). Modulating the thermostability of endoglucanase I from *Trichoderma reesei* using computational approaches. *Protein Engineering, Design & Selection, 28*, 127–135.
11. Liu, J., Yu, H. M., & Shen, Z. Y. (2008). Insights into thermal stability of thermophilic nitrile hydratases by molecular dynamics simulation. *Journal of Molecular Graphics & Modelling, 27*, 529–535.
12. Pikkemaat, M. G., Linssen, A. B. M., Berendsen, H. J. C., & Janssen, D. B. (2002). Molecular dynamics simulations as a tool for improving protein stability. *Protein Engineering, 15*, 185–192.
13. Chen, J., Yu, H. M., Liu, C. C., Liu, J., & Shen, Z. Y. (2012). Improving stability of nitrile hydratase by bridging the salt-bridges in specific thermal-sensitive regions. *Journal of Biotechnology, 164*, 354–362.
14. Colombo, G., & Merz, K. M. (1999). Stability and activity of mesophilic subtilisin E and its thermophilic homolog: insights from molecular dynamics simulations. *Journal of the American Chemical Society, 121*, 6895–6903.
15. Asghari, S. M., Pazhang, M., Ehtesham, S., Karbalaei-Heidari, H. R., Taghdir, M., Sadeghizadeh, M., Naderi-Manesh, H., & Khajeh, K. (2010). Remarkable improvements of a neutral protease activity and stability share the same structural origins. *Protein Engineering, Design & Selection, 23*, 599–606.
16. Inouye, K., Kusano, M., Hashida, Y., Minoda, M., & Yasukawa, K. (2007). Engineering, expression, purification, and production of recombinant thermolysin. *Biotechnology Annual Review, 13*, 43–64.
17. Latt, S. A., Holmquis, B., & Vallee, B. L. (1969). Thermolysin—a zinc metalloenzyme. *Biochemical and Biophysical Research Communications, 37*, 333–339.
18. Mansfeld, J., Vriend, G., Dijkstra, B. W., Veltman, O. R., VandenBurg, B., Venema, G., UlbrichHofmann, R., & Eijsink, V. G. H. (1997). Extreme stabilization of a thermolysin-like protease by an engineered disulfide bond. *Journal of Biological Chemistry, 272*, 11152–11156.
19. Van den Burg, B., Vriend, G., Veltman, O. R., Venema, G., & Eunsink, V. G. H. (1998). Engineering an enzyme to resist boiling. *Proceedings of the National Academy of Sciences, 95*, 2056–2060.
20. Eijsink, V. G. H., Matthews, B. W., & Vriend, G. (2011). The role of calcium ions in the stability and instability of a thermolysin-like protease. *Protein Science, 20*, 1346–1355.
21. O'Donohue, M. J., Roques, B. P., & Beaumont, A. (1994). Cloning and expression in bacillus subtilis of the npr gene from *Bacillus thermoproteolyticus* ROKKO coding for the thermostable metalloprotease thermolysin. *Biochemical Journal, 300*, 599–603.
22. Holland, D. R., Hausrath, A. C., Juers, D., & Matthews, B. W. (1995). Structural-analysis of zinc substitutions in the active-site of thermolysin. *Protein Science, 4*, 1955–1965.
23. Van der Spoel, D., Lindahl, E., Hess, B., Groenhof, G., Mark, A. E., & Berendsen, H. J. C. (2005). GROMACS: fast, flexible, and free. *Journal of Computational Chemistry, 26*, 1701–1718.
24. Hermans, J., Berendsen, H. J. C., Vangunsteren, W. F., & Postma, J. P. M. (1984). A consistent empirical potential for water-protein interactions. *Biopolymers, 23*, 1513–1518.
25. Hess, B., Bekker, H., Berendsen, H. J. C., & Fraaije, J. (1997). LINCS: a linear constraint solver for molecular simulations. *Journal of Computational Chemistry, 18*, 1463–1472.
26. Tang, X. Y., Pan, Y., Li, S., & He, B. F. (2008). Screening and isolation of an organic solvent-tolerant bacterium for high-yield production of organic solvent-stable protease. *Bioresource Technology, 99*, 7388–7392.
27. Kawasaki, Y., Yasukawa, K., & Inouye, K. (2013). Effects of site-directed mutagenesis in the N-terminal domain of thermolysin on its stabilization. *Journal of Biochemistry, 153*, 85–92.
28. Park, H. J., Park, K., Kim, Y. H., & Yoo, Y. J. (2014). Computational approach for designing thermostable *Candida antarctica* lipase B by molecular dynamics simulation. *Journal of Biotechnology, 192*, 66–70.
29. Tian, J., Wang, P., Gao, S., Chu, X., Wu, N., & Fan, Y. (2010). Enhanced thermostability of methyl parathion hydrolase from *Ochrobactrum* sp. M231 by rational engineering of a glycine to proline mutation. *Febs Journal, 277*, 4901–4908.

30. Xie, B.-B., Bian, F., Chen, X.-L., He, H.-L., Guo, J., Gao, X., Zeng, Y.-X., Chen, B., Zhou, B.-C., & Zhang, Y.-Z. (2009). Cold adaptation of zinc metalloproteases in the thermolysin family from deep sea and arctic sea ice bacteria revealed by catalytic and structural properties and molecular dynamics: new insights into relationship between conformational flexibility and hydrogen bonding. *Journal of Biological Chemistry, 284*, 9257–9269.
31. Joo, J. C., Pack, S. P., Kim, Y. H., & Yoo, Y. J. (2011). Thermostabilization of *Bacillus circulans* xylanase: computational optimization of unstable residues based on thermal fluctuation analysis. *Journal of Biotechnology, 151*, 56–65.
32. Joo, J. C., Pohkrel, S., Pack, S. P., & Yoo, Y. J. (2010). Thermostabilization of *Bacillus circulans* xylanase via computational design of a flexible surface cavity. *Journal of Biotechnology, 146*, 31–39.
33. Larsen, D. M., Nyffenegger, C., Swiniarska, M. M., Thygesen, A., Strube, M. L., Meyer, A. S., & Mikkelsen, J. D. (2015). Thermostability enhancement of an endo-1,4-beta-galactanase from *Talaromyces stipitatus* by site-directed mutagenesis. *Applied Microbiology and Biotechnology, 99*, 4245–4253.
34. Kumar, S., Tsai, C. J., & Nussinov, R. (2000). Factors enhancing protein thermostability. *Protein Engineering, 13*, 179–191.
35. Jamil, S., Liu, M.-H., Liu, Y.-M., Han, R.-Z., Xu, G.-C., & Ni, Y. (2015). Hydrophobic mutagenesis and semi-rational engineering of arginine deiminase for markedly enhanced stability and catalytic efficiency. *Applied Biochemistry and Biotechnology, 176*, 1335–1350.
36. Hesampour, A., Siadat, S. E. R., Malboobi, M. A., Mohandesi, N., Arab, S. S., & Ghahremanpour, M. M. (2015). Enhancement of thermostability and kinetic efficiency of *Aspergillus niger* PhyA phytase by site-directed mutagenesis. *Applied Biochemistry and Biotechnology, 175*, 2528–2541.
37. Xu, J., Zhuang, Y., Wu, B., Su, L., & He, B. (2013). Calcium-ion-induced stabilization of the protease from *Bacillus cereus* WQ9-2 in aqueous hydrophilic solvents: effect of calcium ion binding on the hydration shell and intramolecular interactions. *Journal of Biological Inorganic Chemistry, 18*, 211–221.
38. Kim, T., Joo, J. C., & Yoo, Y. J. (2012). Hydrophobic interaction network analysis for thermostabilization of a mesophilic xylanase. *Journal of Biotechnology, 161*, 49–59.
39. Fernandez-Recio, J., Romero, A., & Sancho, J. (1999). Energetics of a hydrogen bond (charged and neutral) and of a cation-pi interaction in apoflavodoxin. *Journal of Molecular Biology, 290*, 319–330.
40. Menach, E., Yasukawa, K., & Inouye, K. (2012). Effects of site-directed mutagenesis of Asn116 in the beta-hairpin of the N-terminal domain of thermolysin on its activity and stability. *Journal of Biochemistry, 152*, 231–239.
41. Nelson, D. L., & Cox, M. M. (2004). *Lehninger principles of biochemistry* (4th ed.). New York: Freeman W.H. & Company.